

## Supplementary information

# Efficient reduced graphene-oxide filter for PM<sub>2.5</sub> removal

*Wonji Jung,<sup>a</sup> Jeong Seok Lee,<sup>a</sup> Seonggeun Han<sup>b</sup>, Seung Hwan Ko<sup>b</sup>, Taewoo Kim<sup>\*c</sup>  
and Yong Hyup Kim<sup>\*a</sup>*

<sup>a</sup> School of Mechanical and Aerospace Engineering, Seoul National University, Seoul 08826, South Korea

<sup>b</sup> Nano and Thermal Science Lab, Department of Mechanical Engineering, Seoul National University, Seoul 08826, Korea

<sup>c</sup> Department of Mechanical Engineering, Incheon National University, Incheon, 22012, South Korea

E-mail: [taewoo.kim@inu.ac.kr](mailto:taewoo.kim@inu.ac.kr), and [yongkim@snu.ac.kr](mailto:yongkim@snu.ac.kr)

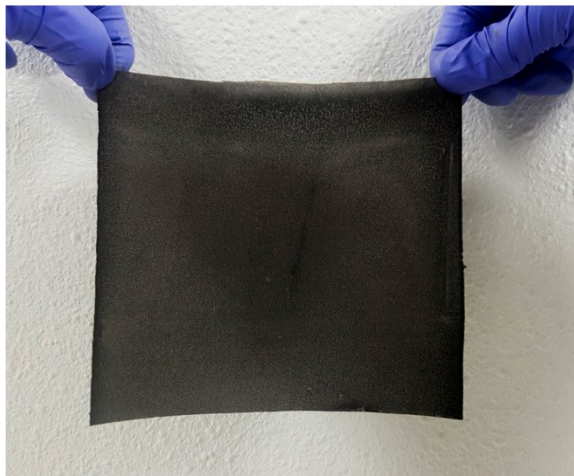


Fig. S1 The optical image of large IMA-rGO filter.

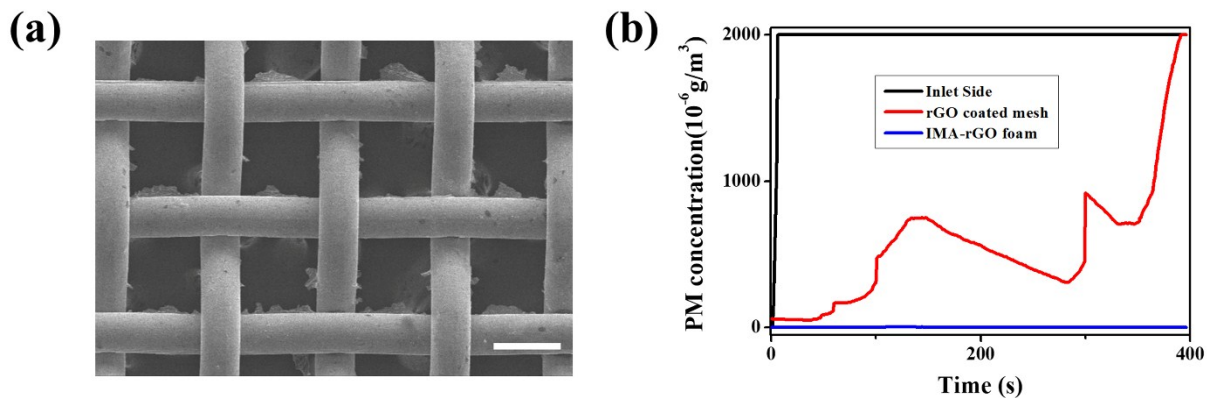


Fig. S2 Comparison of rGO-coated mesh and IMA-rGO foam: (a) Scanning Electron Microscopy (SEM) image of rGO coated mesh (Scale bar is 300  $\mu\text{m}$ ). (b) Experimental PM removal result with rGO-coated mesh and IMA-rGO (Ion-mediated assembled reduced graphene oxide) foam.

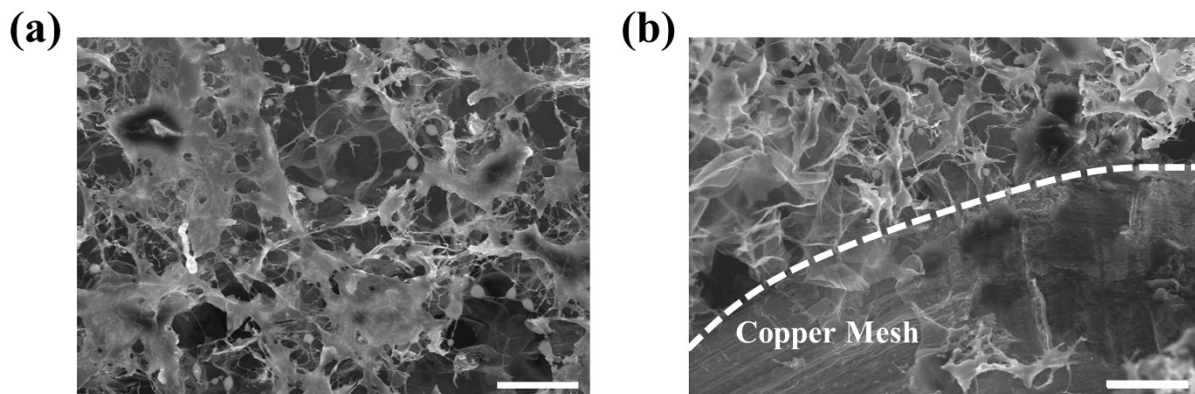


Fig. S3 Cross sectional SEM image of IMA-rGO filter after PM<sub>2.5</sub> removal test: (a) The middle part of cross section (Scale bar is 20 μm). (b) The bottom part of cross section (Scale bar is 20 μm).

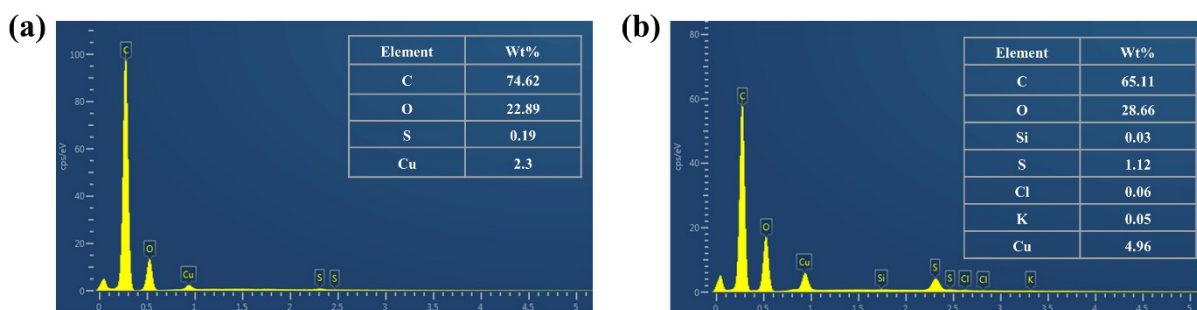


Fig. S4 Energy-Dispersive X-ray (EDX) analysis result of IMA-rGO filter: (a) before and (b) after PM<sub>2.5</sub> removal test.

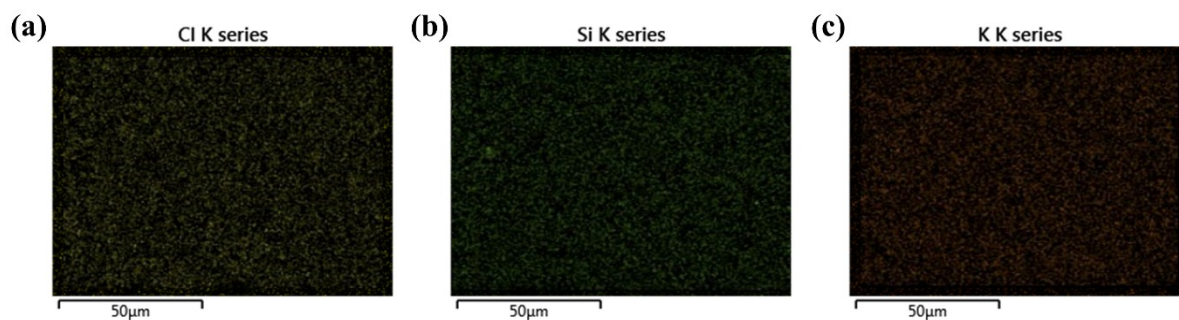


Fig. S5 EDX mapping analysis result of IMA-rGO filter after  $PM_{2.5}$  removal test: Mapping result for (a) chloride, (b) silicon, and (c) potassium.

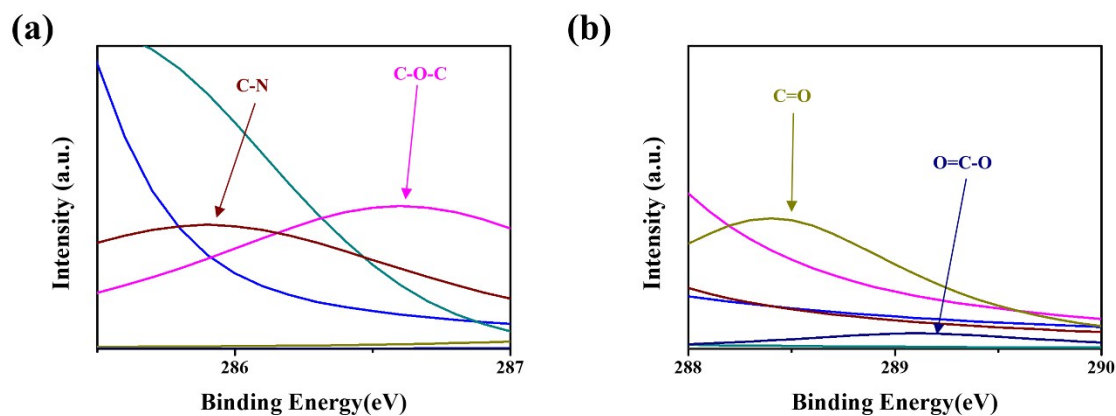


Fig. S6 Partial results of X-Ray Photoemission (XPS) analysis of IMA-rGO filter after PM removal (excerpt from Fig. 3d): (a) Enlarged graph of the binding energy from 285.5 to 287. (b) Enlarged graph of the binding energy from 288 to 290.

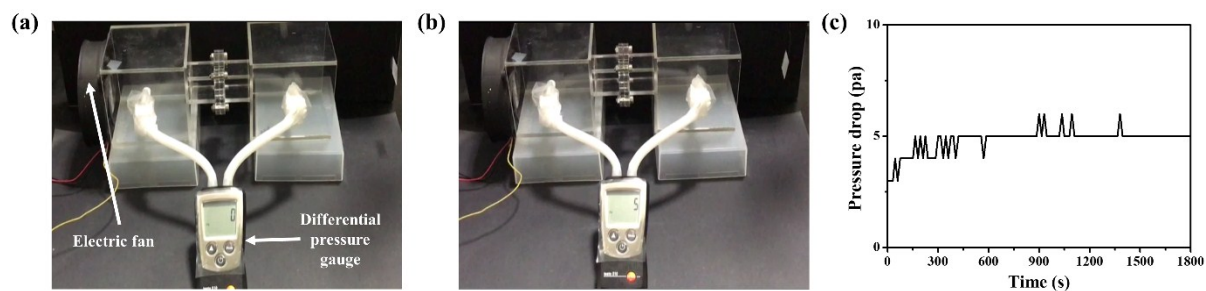


Fig. S7 Optical image of pressure drop test result: (a) Pressure drop test result of control sample. (b) Pressure drop test result of IMA-rGO filter. Air flow rate is 1.1 m/s for both cases. (c) The result of time-dependent pressure drop test of IMA-rGO filter.

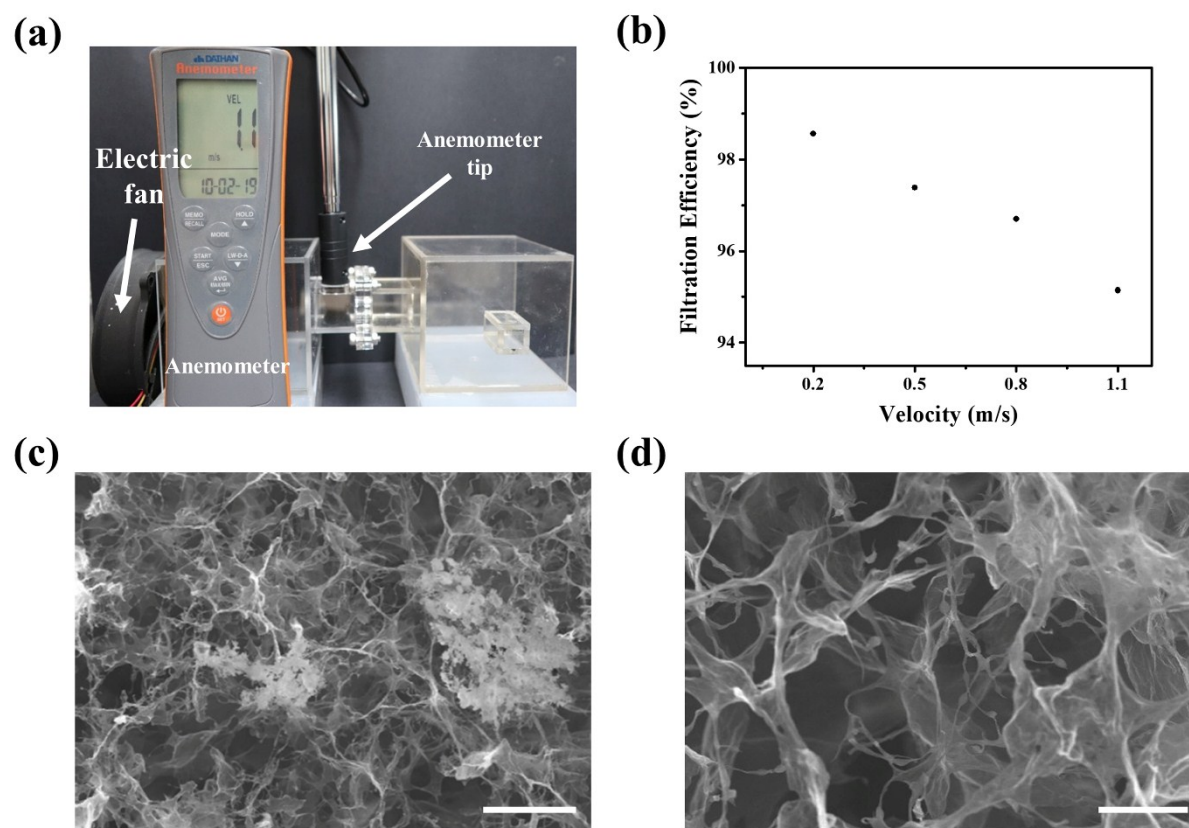


Fig. S8  $PM_{2.5}$  removal test under the air flow: (a) Optical image of experimental setup and anemometer. (b) Result of PM removal performance according to air flow rate. (c) SEM image of the filter surface after PM removal (Scale bar is 20  $\mu m$ ). (d) More magnified SEM image of the filter surface after PM removal (Scale bar is 5  $\mu m$ ).

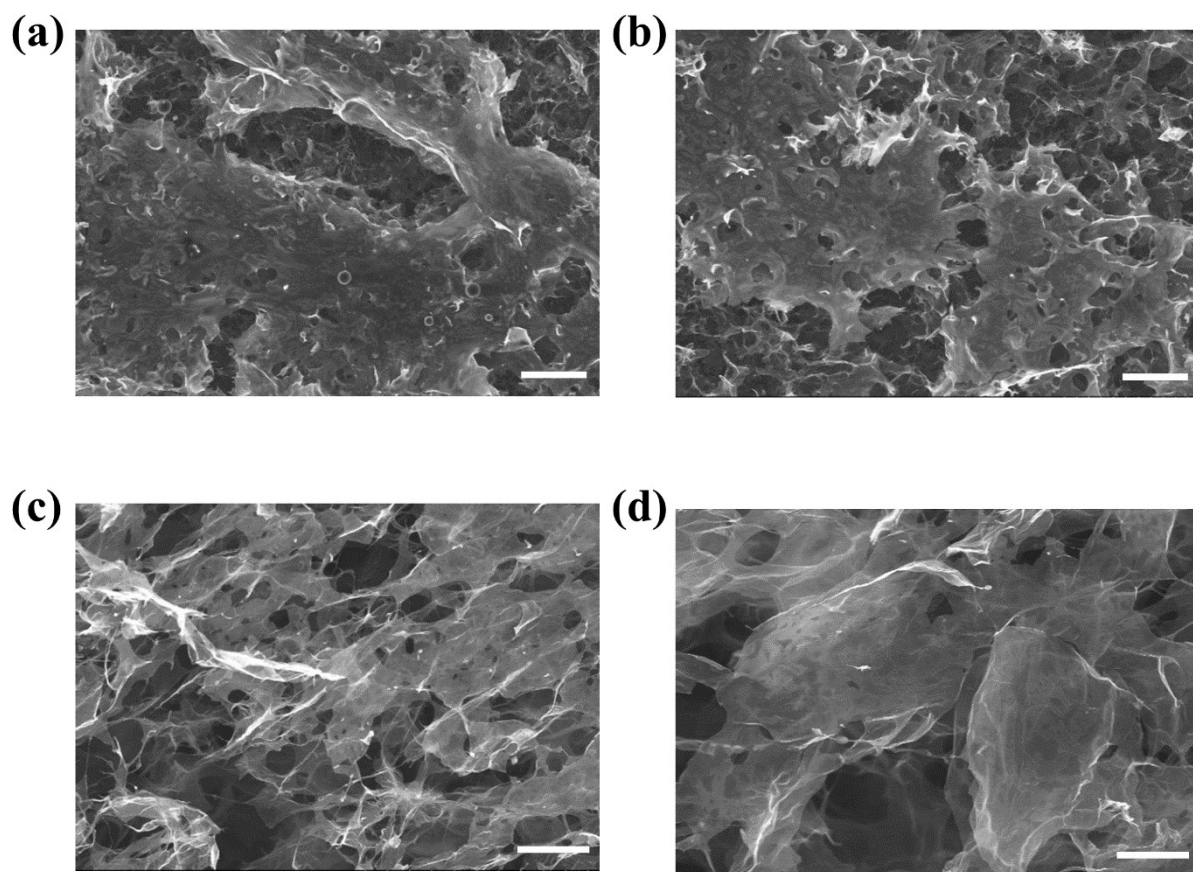


Fig. S9 SEM image of IMA-rGO filter after indoor air purification experiment that simulating the real environment: (a and b) SEM image of surface that adjacent to the outdoor cell air (Scale bar is 50  $\mu\text{m}$ ). (c) SEM image of surface adjacent to the indoor cell air (Scale bar is 10  $\mu\text{m}$ ). (d) More magnified SEM image of surface adjacent to the indoor cell air (Scale bar is 5  $\mu\text{m}$ ).

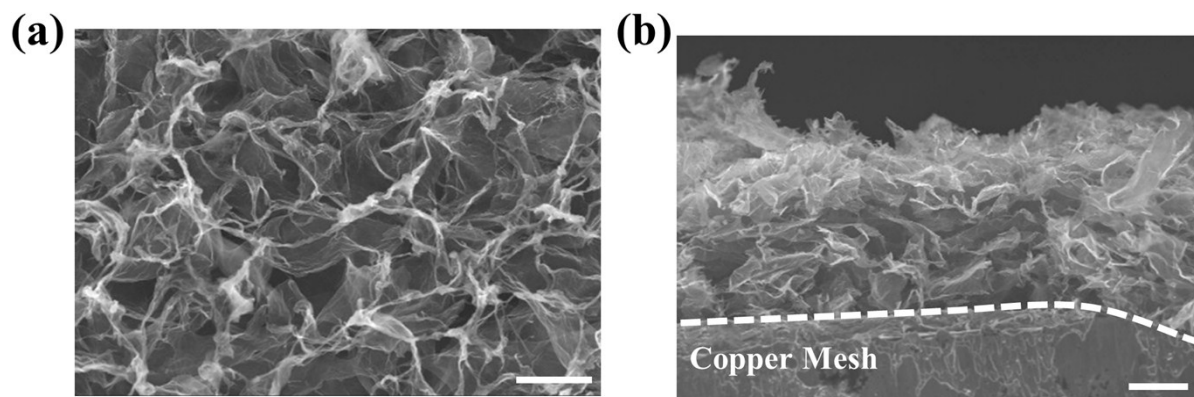


Fig. S10 SEM image of IMA-rGO filter after cleaning process: (a) SEM image of the surface of the filter. (Scale bar is 10  $\mu\text{m}$ ). (b) SEM image of the cross section of the filter. (Scale bar is 20  $\mu\text{m}$ ).